Langmuir−Blodgett Films of Poly(3-hexylthiophene) Doped with the Endohedral Metallofullerene Dy@C_{82}: Preparation, Characterization, and Application in Photoelectrochemical Cells

Shangfeng Yang, Louzhen Fan, and Shihe Yang*

Department of Chemistry, The Hong Kong University of Science and Technology, Clear Water Bay, Kowloon, Hong Kong

Received: November 22, 2003; In Final Form: January 24, 2004

We have successfully constructed photoelectrochemical (PEC) cells based on the Langmuir−Blodgett (LB) films of poly(3-hexylthiophene) (P3HT) doped with Dy@C_{82}. The composite structure is featured by the interaction between Dy@C_{82} and the thiophene building blocks of P3HT, which take an edge-on arrangement at the air/water interface. The usage of the P3HT−Dy@C_{82} composite LB films in photoelectrochemical (PEC) cells yields a dramatic enhancement of the cathodic photocurrent, with the power-conversion efficiency (η_e) and quantum yield (Φ) being up to 16-fold and 9-fold higher, respectively, than those of pure P3HT cells. This is attributed to the facile photoinduced electron transfer between P3HT and Dy@C_{82}, which is also revealed by photoluminescence (PL) spectroscopic characterization. The optimum PEC performance is found to be correlated with an ordered film structure as revealed by AFM measurements. The effects of the electron acceptor, bias voltage, light intensity, and number of layers have been studied in detail. Comparison studies have also been conducted with bilayer PEC cells and PEC cells in which Dy@C_{82} is replaced by C_{60}. A possible mechanism for the cathodic photocurrent generation is proposed on the basis of these studies.

Introduction

The stability and processibility of some conducting polymers such as head-to-tail polythiophene are attractive for active electronic components in various thin-film devices and sensors.[1,2] For example, photovoltaics (PVs) derived from such thin plastic films hold great technological potential as a cost-effective, renewable alternative energy source.[3] Photoelectrochemical (PEC) cells based on conducting polymers with nanocrystal dopants are quite promising because these offer the prospect of cheap fabrication together with other attractive features such as flexibility.[4,5] For the fabrication of ordered ultrathin films with well-defined architecture, the Langmuir−Blodgett (LB) technique offers a unique approach.[6−8] The application of the LB technique to conjugated polymers such as polythiophene has produced a variety of electrical and optical ultrathin film devices including field-effect transistors (FET) and light-emitting diodes (LED).[6,7]

The utilization of fullerene derivatives for developing novel nanodevices requires robust films on desired electrode surfaces with well-defined morphology.[9] Recently, PEC cells containing fullerenes have emerged as a new generation of PV devices with enhanced efficiency.[4,10] Endohedral metallofullerenes represent a special member of the fullerene family, and the encapsulated metal atoms bring about many new properties.[11] For example, the mono-metallofullerenes M@C_{82} (M = lanthanide elements) possess not only greater electron-accepting ability but also stronger electron donating power than C_{60},[12] which may be harnessed to construct PV or PEC cells with enhanced photoelectric energy conversion.

During the past few years, we have taken part in constructing LB films of metallofullerenes and their mixtures with various molecules. There are at least two anticipated roles of the mixed molecules. First, they are used to direct the assembly of the metallofullerene species. Second, they themselves may be electroactive and/or photoactive and can participate in the charge-separation processes. For the LB films of Dy@C_{82} mixed with long-chain arachidic acid (AA),[13,14] we obtained a higher anodic photocurrent quantum yield (~3.9%) than for the pure Dy@C_{82} films and the C_{60}−AA mixture films on ITO under appropriate conditions.[13] More recently, by mixing metallofullerene Dy@C_{82} with metallophthalocyanines (MPcs), thin films of new donor−acceptor-type complexes [Pc−metallofullerene] were successfully constructed, exhibiting anodic photocurrent quantum yields of up to 7−8%.[15]

In this paper, we report the first successful construction of the LB film of poly(3-hexylthiophene) (P3HT) doped with Dy@C_{82} and the first systematic PEC study of this film. P3HT is chosen because of its (1) good film-formation properties,[6,7] (2) p-type semiconductor character,[5c,d] and (3) excellent PV performance.[16] The LB technique not only allows us to control the molecular arrangements in the ultrathin films but also places fewer demands on the number of samples, which are particularly important for the exotic metallofullerenes. Molecular arrangements in the P3HT−Dy@C_{82} Langmuir films are deduced by studying the $\pi-A$ isotherms obtained with a series of spreading solutions with different molar ratios of P3HT/Dy@C_{82}. A dramatic enhancement of the cathodic photocurrent has been demonstrated for the P3HT−Dy@C_{82} PEC cells.[17] The correlation between the optimum PEC performance with the ordered film structure is revealed by the AFM measurements. We have carried out comprehensive studies of the effects of the electron acceptor, bias voltage, light intensity, number of layers, film structures, and substitution of Dy@C_{82} by C_{60} on the PEC performance in order to understand the photocurrent-

* Corresponding author. E-mail: chsyang@ust.hk.

10.1021/jp0375618 CCC: $27.50
Published on Web 03/17/2004

generation mechanism. In the following text, we will first describe our experimental procedures. Then the LB film deposition and optical characterization are presented, followed by the exposition of the PEC results. Finally, concluding remarks will be given.

Experimental Section

Materials and Reagents. High-purity Dy@C_{82} and C_{60} were prepared by a combination of standard dc arc discharge and HPLC separation.[18] Poly(3-hexylthiophene-2,5-diyl) (regioregular, $\bar{M}_w \approx 87\,000$) was purchased from Aldrich. KCl (Riedel-De Haen AG) was used as an electrolyte for the PEC measurements in water. Methyl viologen dichloride (MV^{2+}) (Acros Organics Co.) was used as an electron acceptor. Deionized water, which had been purified by passing through an EASYpure compact ultrapure water system (Barnstead Co.), was used in all of the experiments reported in this paper.

Preparation and Characterization of LB Films. A Langmuir minitrough (Applied Imaging, U.K.) was employed for the preparation of the films. The air/water interface was thoroughly cleaned by complete barrier movement to ensure that the maximum surface-pressure difference was less than 0.2 mN·m^{-1} upon compression. The subphase was ultrapure water (25 ± 1 °C, pH 6.50, ρ = 18.3 MΩ·cm). A series of spreading solutions with different molar ratios of P3HT(monomer)/Dy@C_{82} (C_{60}) ([P3HT] (monomer) ≈ (3−4) × 10^{-5} mol·dm^{-3}, in toluene) were prepared to investigate the composition dependence of the Langmuir films. A known volume of the P3HT−Dy@C_{82} (4−5 mL) solution was carefully spread onto the surface of the clean water subphase (505 cm^2) dropwise using a 0.5-mL syringe. This procedure lasted for over 1 h. After the solvent had evaporated completely (>30 min), the spreading molecules at the air/water interface were compressed at a barrier speed of 1 cm/min, and the surface-pressure−area (π−A) isotherm was recorded. LB films with odd number of layers of P3HT−Dy@C_{82} (C_{60}) were deposited from the air/water interface by vertical dipping onto a transparent indium−tin oxide (ITO) glass substrate (10 × 15 mm^2, R_s = 85 Ω/square, Delta Technologies Ltd., Stillwater, MN) or quartz plate (10 × 15 mm^2, Electronic Space Products International, Ashland, OR) that had been hydrophilically pretreated.[13,15] For LB films with even numbers of layers, the substrates were hydrophobically pretreated with 1,1,1,3,3,3-hexamethyldisilazane (Aldrich).[19] The LB deposition was carried out at a dipping rate of ∼0.9 mm/min under a constant surface pressure of 20 mN·m^{-1}. UV−vis absorption spectra were recorded with a Milton Roy spectrometer (Spectronic 3000). For polarized UV−vis spectroscopy, a polarizer was placed before the sample. Photoluminescence (PL) spectra were recorded on monolayer films on quartz using an argon ion laser (488 nm) as the excitation light source at room temperature. The emitted light was collected and dispersed by the Spex500M spectrometer. A photomultiplier tube working in the photon-counting mode was used as the detector.

Monolayer LB films of P3HT−Dy@C_{82} with different molar ratios were also deposited on freshly cleaved mica surfaces for atomic force microscopy (AFM) measurements, which were carried out using a Nanoscope III multimode AFM (Digital Instruments) operated in the tapping mode under ambient conditions.

Photoelectrochemical Measurements. The PEC experiments were performed with a model 600 electrochemical analyzer (CH Instruments Inc.) in a three-electrode configuration under ambient conditions. The P3HT−Dy@C_{82} (C_{60}) LB films on the ITO substrate were used as working electrodes, which were

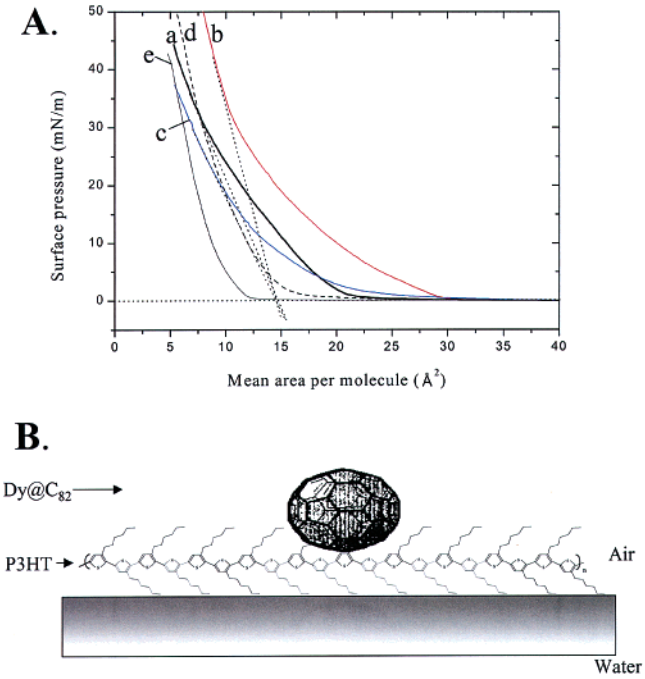

Figure 1. (A) Surface pressure−area (π−A) isotherms of P3HT−Dy@C_{82} (a−c), pure P3HT (d), and P3HT−C_{60} (e) at the air/water interface at pH 6.5. The molar ratios of P3HT/Dy@C_{82} (C_{60}) are 20:1 (a), 10:1 (b), 40:1 (c), and 25:1 (e). The barrier-compression speed is 2 cm·min^{-1}. (B) Possible molecular structures of the P3HT/Dy@C_{82} (20:1) Langmuir film.

illuminated through the substrate/electrode interface (SE). A Pt wire and Ag/AgCl were used as the counterelectrode and the reference electrode, respectively. The electrolyte was an aqueous solution of KCl with a concentration of 0.1 mol·dm^{-3} (pH 6.5). A 1000-W xenon lamp (Oriel) was used as the light source. To minimize thermal effects, a homemade water filter was placed before the PEC cell. The light intensity was calibrated with a power meter (Newport Co.), but no corrections were made for the reflections. For white-light illumination, an optical filter (400FH90-25, Andover Corp.) was used to cut off the light with λ < 400 nm. For narrow-band illumination, the light ($\Delta\lambda \approx 10$ nm at the exit slit) was obtained with a monochromator (Triax 190, Instruments S.A. Inc.). For each set of preparation conditions for the LB films on ITO, more than six samples were measured to ensure the reproducibility of the photocurrent data.

Results and Discussion

A. Preparation and Characterization of Langmuir−Blodgett Films. *Formation of Langmuir−Blodgett Films.* The P3HT−metallofullerene system that we studied forms stable Langmuir monolayer films under our experimental conditions, as evidenced by the reversibility and reproducibility of the π−A isotherms in the compression−expansion cycles. At the molar ratio of P3HT/Dy@C_{82} = 20:1 or the weight ratio of 2.9:1, the π−A isotherm displays a steep pressure increase in the condensed-phase region, and no sign of film collapse was observed even when the surface pressure reached ∼45 mN·m^{-1} (curve a in Figure 1A). By extrapolating the condensed-phase region of the π−A isotherm to zero pressure, the mean limiting area per molecule ($A_{limiting}$) is estimated to be 14.7 Å^2/molecule. For comparison, π−A isotherms with other molar ratios of P3HT/Dy@C_{82} are also shown in Figure 1A (curves b and c), and the $A_{limiting}$ data are summarized in Table 1. Although the molar ratio of P3HT/Dy@C_{82} affects the $A_{limiting}$ value only slightly, the isotherm is more sensitive to it, and a higher

TABLE 1: Characteristics of the Langmuir Monolayers and LB Films

film composition	ratio[a] mol	ratio[a] wt	mean $A_{limiting}$ (Å^2/molecule)[b]	dichroic ratio (R)[c]	order parameter (O)[d]
pure P3HT	100:0	100:0	11.8	1.22	0.07
P3HT−Dy@C_{82}	10:1	1.4:1	14.5	1.37	0.11
	15:1	2.2:1	14.2	1.19	0.06
	20:1	2.9:1	14.7	1.40	0.12
	25:1	3.6:1	14.5	1.29	0.09
	30:1	4.3:1	14.4	1.25	0.08
	40:1	5.8:1	14.5	1.12	0.04
P3HT−C_{60}	10:1	1.4:1	13.8	1.11	0.04
	15:1	2.2:1	10.3	1.21	0.07
	20:1	2.9:1	10.5	1.13	0.04
	25:1	3.6:1	10.1	1.40	0.12
	30:1	4.3:1	10.9	1.19	0.06
	40:1	5.8:1	11.5	1.08	0.03

[a] Ratio of P3HT(unit): Dy@C_{82}. mol: molar; wt: weight (wt ratio = mol ratio × 166/1146.5). [b] The limiting area per molecule ($A_{limiting}$) is the mean value based on three compression−expansion cycles. [c] R is defined as the ratio of s-polarized absorbance to p-polarized absorbance (at 520 nm). (See the text for the definitions of s and p polarization.) [d] O is defined as $(R - 1)/(R + 2)$. See also refs 6a and 20.

concentration of Dy@C_{82} brings the liquid-expanded to liquid-condensed phase transition to a higher surface pressure.

As a reference, the Langmuir film of pure P3HT (curve d in Figure 1A) prepared under the same conditions as for the composite films gives a limiting monomer area (A_{mono}) of 11.8 Å^2/molecule. This value is in good agreement with that reported by Xu et al.,[6a] indicating that the backbones of P3HT take an edge-on arrangement in the film (i.e., the main polymer chain is parallel to the air/water interface with the thiophene rings standing vertically (see Figure 1B and C)). A similar molecular arrangement has been proposed for the Langmuir films of other polythiophenes.[8] The measured A_{mono} is slightly smaller than the ideal surface area of the thiophene unit (14.5 Å^2) by assuming a close-packed monolayer,[6a] suggesting a certain extent of interchain interactions. In addition, the measured A_{mono} is also dependent on the spreading solvent (e.g., A_{mono} with toluene is larger than those with xylene and chloroform, as also found by other researchers because of more severe aggregations for the latter[6a,7a]).

The fact that nearly constant mean limiting molecular areas are obtained in the composite films irrespective of the variation of the molar ratio of P3HT/Dy@C_{82} suggests that the same molecular arrangement is taken as in the pure P3HT film. Furthermore, because the $A_{limiting}$ values for the P3HT−Dy@C_{82} films are quite close to the ideal area of the thiophene unit (14.5 Å^2), it is deemed reasonable that the Dy@C_{82} molecules are sitting on the thiophene units of P3HT, perhaps with a certain extent of intercalation into the polymer. Such a molecular arrangement, which is especially relevant for the more ordered P3HT−Dy@C_{82} (20:1) film (see curve a in Figure 1A), is illustrated in Figure 1B.

Usually, the Dy@C_{82} molecules tend to aggregate in Langmuir films because of the strong dipolar and hydrophobic interactions.[13,14] P3HT alone aggregates as well.[6a] This underscores the significance of the present P3HT−Dy@C_{82} system—the mutual and synergetic inhibition of the aggregation of both the metallofullerene and the P3HT constituents.

For comparison, the π−A isotherm of a P3HT−C_{60} Langmuir film (P3HT/C_{60} = 25:1) is also shown in Figure 1A (curve e).

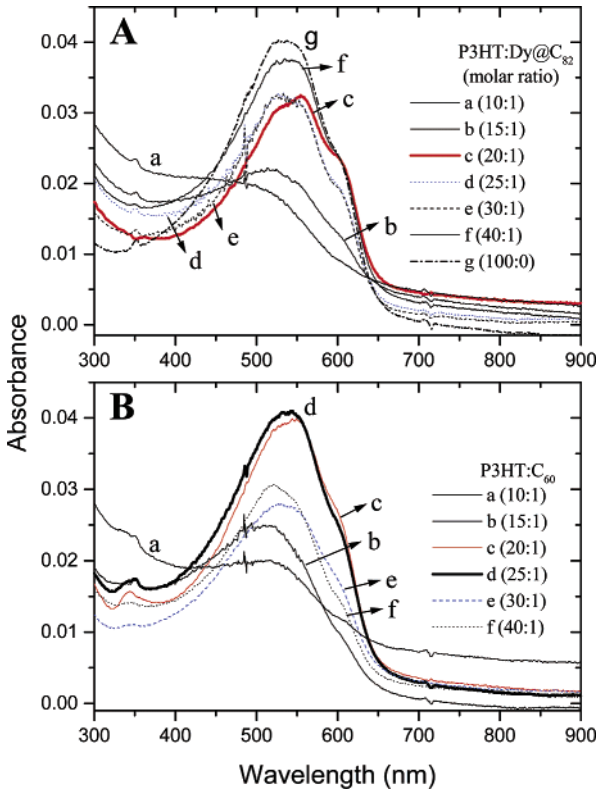

Figure 2. UV−vis absorption spectra of the P3HT−Dy@C_{82} (A) and P3HT−C_{60} (B) monolayer LB films on quartz plates. The spectrum of pure P3HT is also shown as a reference (curve g in A).

It appears to be similar to those of the P3HT−Dy@C_{82} films except that the $A_{limiting}$ value is a bit smaller (10.1 Å^2/molecule) (Table 1). It is noteworthy that the $A_{limiting}$ value is even smaller than the measured monomer area except for the case at P3HT/C_{60} = 10:1, presumably because the interactions between the C_{60} and the P3HT molecules are somewhat weaker and thus are not as effective as in the case of Dy@C_{82} in inhibiting the self-aggregation of these molecules.

Absorption Spectra. Monolayer films of both P3HT−Dy@C_{82} (C_{60}) and pure P3HT were easily transferred onto a hydrophilic ITO substrate or quartz plate by vertical dipping (upstroke) with a transfer ratio of ~1. Figure 2 shows the UV−vis absorption spectra of the P3HT−Dy@C_{82} (A) and P3HT−C_{60} (B) monolayer LB films on quartz plates together with that of P3HT (curve g in A) for reference. The spectrum of pure P3HT shows a broad absorption feature arising from the π−π* transition with three bumps at 520, 555, and 606 nm. This is in good agreement with the previous results and conforms to the well-ordered structure of the film.[6a] Clearly, the spectra of the P3HT−Dy@C_{82} (C_{60}) films are simply the spectral sums of the individual components (i.e., P3HT and Dy@C_{82} (C_{60})). Except for the case of P3HT/Dy@C_{82} (C_{60}) = 10:1 (curves a), doping with Dy@C_{82} (C_{60}) hardly modifies the absorption characteristics of P3HT, which rules out the possibility of significant ground-state charge transfer between P3HT and Dy@C_{82} (C_{60}).

Further information on the molecular arrangements in the LB films has been obtained by polarized electronic absorption spectroscopy as shown in Figure 3 for P3HT (A), P3HT−Dy@C_{82} (B), and P3HT−C_{60} (C). Apparent dichroism for the absorption arising from the π−π* transition at the incident angle of 0° is detected. The dichroic ratio R is defined as A_s/A_p, where A_s and A_p are the absorbances of the film obtained for polarized light with the electric vector parallel (s polarization) and perpendicular (p polarization) to the dipping direction, re-

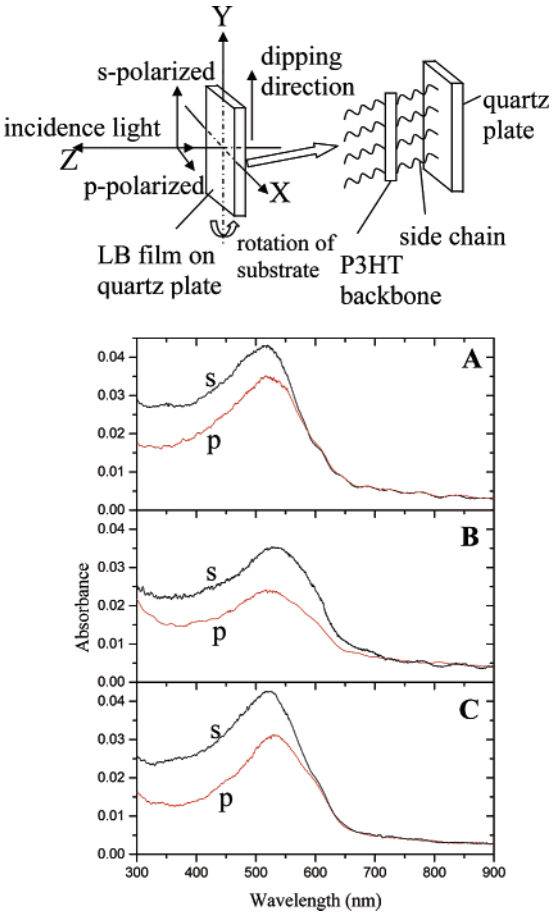

Figure 3. Polarized UV−Vis absorption spectra of pure P3HT (A), P3HT−Dy@C_{82} (20:1) (B), and P3HT−C_{60} (25:1) (C) monolayer LB films on quartz plates with an incident angle of 0°. A schematic representation of the experimental setup for the polarized UV−vis absorption measurements is given in the top panel.

spectively.[6a,15,19,20] The degree of order of the P3HT backbone is evaluated by calculating the dichroic ratio (*R*) and order parameter (*O*) for the films prepared under different conditions as summarized in Table 1. For pure P3HT, our measured *R* is comparable to that reported in ref 6a (1.10−1.60), confirming that the same edge-on conformation of the polymer backbone is taken in the LB films. However, the structural anisotropies of the LB films of P3HT−Dy@C_{82} and P3HT−C_{60} are found to be composition-dependent, with a maximum of *R* for P3HT/Dy@C_{82} = 20:1 and for P3HT/C_{60} = 25:1. This implies pronounced differences in the in-plane ordering of the P3HT molecules in the composite films, which will be further discussed below in conjunction with the PEC data.

Monolayer LB films were studied by steady-state photoluminescence (PL), and the data are shown in Figure 4 for P3HT−Dy@C_{82} (A) and P3HT−C_{60} (B) on quartz plates together with that of P3HT. The pure P3HT monolayer exhibits very broad PL bands at ∼651 nm (1.90 eV) and ∼698 nm (1.78 eV), in good agreement with a previous LB film study.[21a] However, the peaks are both slightly blue-shifted from those reported for the casting films.[21b,c] When doped with Dy@C_{82} or C_{60}, the PL of P3HT is dramatically quenched, and the quenching effect is also composition-dependent. Conceivably, photoinduced change transfer has occurred between the two components, which may compete with the radiative emission of P3HT.[22,23] This is a sought-after feature for photoelectrochemical (PEC) cells, as will be presented below. It should be mentioned that the PL peaks of P3HT do not show noticeable blue shifts upon

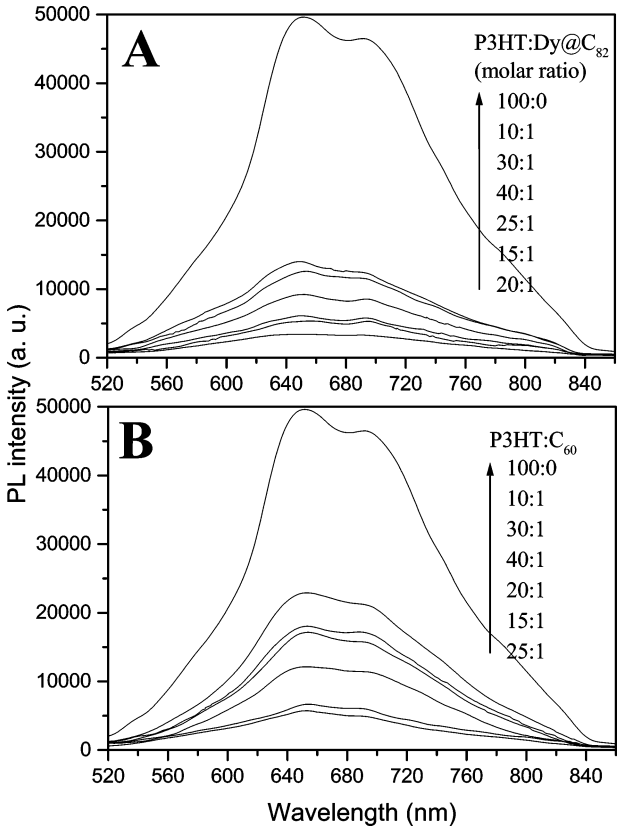

Figure 4. Photoluminescence (PL) spectra of the P3HT−Dy@C_{82} (A) and P3HT−C_{60} (B) monolayer LB films on quartz plates. The spectrum of pure P3HT is also shown as a reference.

fullerene or metallofullerene encapsulation, as found for the (PAT-18)−C_{60} and (MEH−PPV)−C_{60} systems.[24]

Multilayers of P3HT−Dy@C_{82} were transferred to both hydrophilic and hydrophobic substrates in a layer-by-layer fashion by vertical deposition. The transfer ratio for the downstrokes (0.1−0.2) is much smaller than that of the upstrokes (∼1). Similar to the [Dy@C_{82}−MPc] system, the poor transfer for the downstrokes is presumably due to the hydrophobicity of the molecules, which are unwilling to enter the water subphase.[15] As reported by Xu et al., the LB films of pure P3HT did not adhere well to substrates during vertical deposition, so the horizontal deposition method had to be used instead.[6a] Despite the poor transfer for the downstrokes, we have successfully built up P3HT−Dy@C_{82} multilayers using the vertical deposition method by attending to the careful pretreatment of the substrates. Figure 5 shows the UV−vis absorption spectra of the P3HT−Dy@C_{82} (20:1) LB films on quartz as a function of the number of layers up to 15. Good linearity between the absorbance at 555 nm and the number of layers is obtained for multilayers up to seven (see inset), indicating that LB films of different thicknesses deposited on the quartz substrates are quite uniform. However, the film-transfer behavior becomes worse with further increases in the number of layers because of the hydrophobicity of the molecules, as mentioned above.

B. Photoelectric Response of the P3HT−Dy@C_{82} (C_{60}) Films on ITO Electrodes. *Action spectrum.* Figure 6 shows the photocurrent action spectrum for a P3HT−Dy@C_{82} (20:1) monolayer on ITO along with its absorption spectrum. Because the absorption of ITO increases sharply below 340 nm, the photocurrent action spectrum was recorded only at wavelengths above 400 nm where background photocurrents from ITO are negligible. Obviously, the photocurrent spectrum coincides well

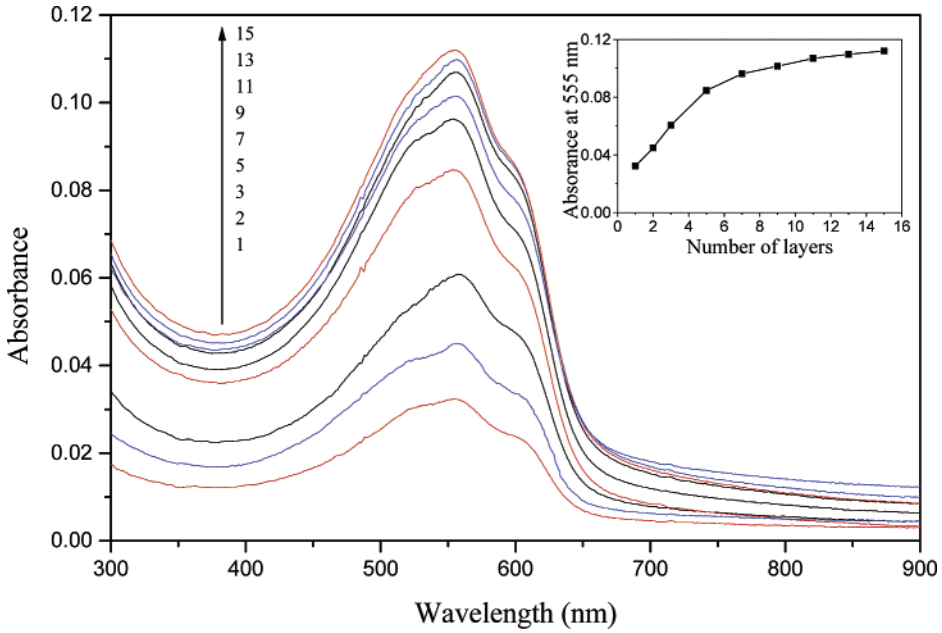

Figure 5. UV−vis absorption spectra of the P3HT−Dy@C_{82} (20:1) multilayer LB films on quartz plates as a function of the number of layers. (Inset) Absorbance at 555 nm as a function of the number of layers.

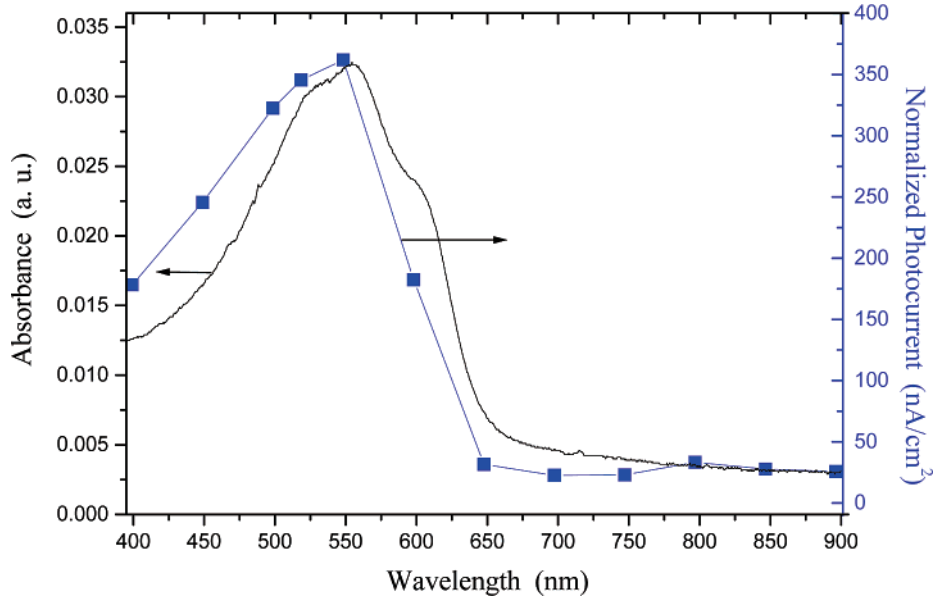

Figure 6. Action spectrum (solid squares) of the cathodic photocurrents (0.1 mol·dm^{-3} KCl electrolyte solution, [MV^{2+}] = 8.0 mmol·dm^{-3}, no bias voltage) and absorption spectrum (solid line) of the monolayer of P3HT−Dy@C_{82} (20:1) on ITO. The photocurrents are normalized to the incident-light intensity at different wavelengths.

with the corresponding absorption spectrum, suggesting strongly that the photoabsorption of P3HT and/or Dy@C_{82} in the LB films is responsible for photocurrent generation.

Effect of the Electron Acceptor. O_2 is known to act as an electron acceptor through the formation of a superoxide anion radical ($O_2^{\bullet -}$) for many photoactive molecules including polythiophenes.[5c,25] However, it is reported that O_2 quenches the excited state of Dy@C_{82} and the triplet state of C_{60} as O_2 is raised from the triplet ground state to the singlet excited state.[13] Hence, it would be interesting to see the effect of O_2 on photocurrent generation in the P3HT−Dy@C_{82} (C_{60}) systems. Figure 7A shows the photocurrent traces under ambient conditions (a) and in the absence of oxygen (N_2 gas was used to degas O_2 in the electrolyte solution) (b) for the P3HT−Dy@C_{82} (20:1) monolayer film. It is significant that the cathodic photocurrent response is enhanced by a factor of ∼1.4 in the presence of O_2. We also found that the P3HT−C_{60} and the pure P3HT films exhibit comparable photocurrent enhancement due to O_2. This implies that O_2 mainly interacts with the photoexcited P3HT by accepting an electron instead of quenching the excited states of Dy@C_{82} or C_{60}. Several reasons can be recognized. First, P3HT is more abundant in the mixture film. Second, P3HT is a better absorber in the visible region, as evidenced by the UV−vis spectra (Figure 2). Third, P3HT is a good electron donor. We noticed that there is photocurrent degradation, which is known for P3HT when irradiated in the form of thin films or dissolved in nonaqueous solvents containing dissolved molecular oxygen.[5b,d,26]

Figure 7B plots the photocurrent (I_{ph}) versus bias voltage from −0.20 to 0.70 V (vs Ag/AgCl) for the monolayer films of P3HT−Dy@C_{82} (20:1) at different pH values under white-light illumination (∼354 mW/cm^2). Both the cathodic photocurrent

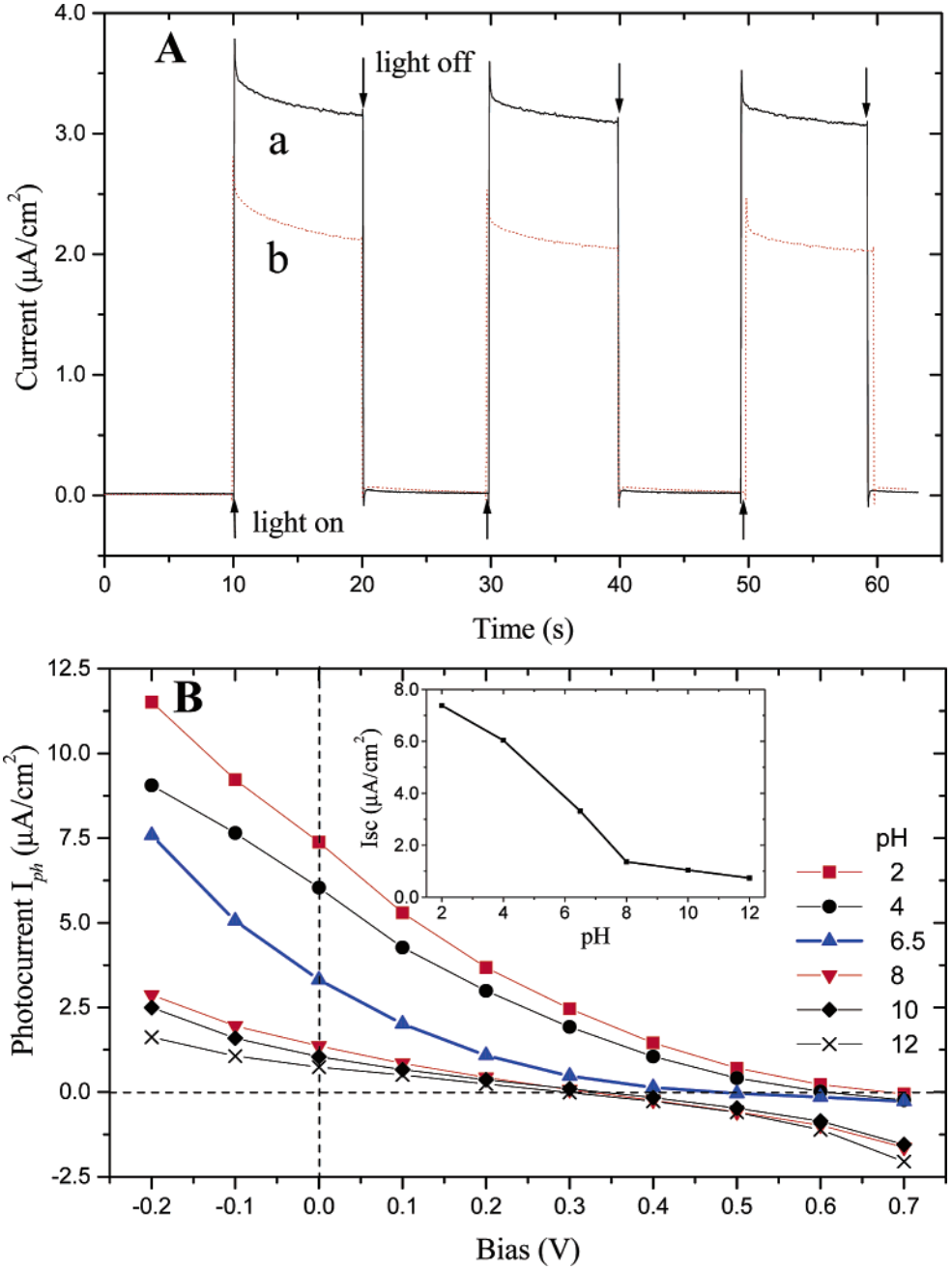

Figure 7. (A) Effect of O_2 on the photocurrent responses of the P3HT−Dy@C_{82} (20:1) monolayer on ITO electrodes under ambient conditions (solid line, curve a) and under an N_2 atmosphere (dotted line, curve b) (0.1 mol·dm^{-3} KCl electrolyte solution, pH 6.5, no MV^{2+}, no bias voltage). The arrows indicate the light on−off cycles. (B) Effect of pH on the photocurrent responses of the P3HT−Dy@C_{82} (20:1) monolayer on ITO electrodes (0.1 mol·dm^{-3} KCl electrolyte solution, no MV^{2+}, intensity of white light = 354 mW·cm^{-2}). (Inset) Dependence of the short-circuit current (I_{sc}) on pH.

and its onset potential (V_{oc}) increase with the decreasing pH of the solution. We attribute this to the stronger electron-accepting ability of O_2 in an acidic solution than in an alkaline solution, which enhances the cathodic photocurrent generation.[27] El-Rashiedy et al. reported a PEC study of relatively thicker films prepared by casting. By changing the pH from 12 to 2, they observed a photocurrent increase by only a factor of 2; furthermore, the onset potential remained constant. On the basis of these results, the absence of Fermi-level pinning was concluded.[5d] Our system is quite different in that (1) the redox couple of $O_2/O_2^{\bullet-}$ instead of H_2O/H_2 should be taken into consideration[5c,25] and (2) the flat band potentials (E_{FB}) of our film electrodes are generally smaller because of the monolayer nature of the LB films, as will be discussed below. Nevertheless, this result further reveals the effects of O_2 as an acceptor. Furthermore, it is likely that Fermi-level pinning occurs in our system and can be mitigated by tuning the pH value of the solution.

Because the concentration of O_2 is limited and difficult to control, we researched another effective electron acceptor—methyl viologen (MV^{2+}).[25] As can be seen from Figure 8, the cathodic photocurrent for the P3HT−Dy@C_{82} (20:1) monolayer film under white-light illumination increases sharply with the increasing concentration of MV^{2+}, then starts to level off at $[MV^{2+}] \approx 2$ mmol/dm^3, and finally reaches an enhancement factor of up to ~2.3. Clearly, the introduction of MV^{2+} increases and stabilizes the photocurrent response. (See the inset, and compare with that in Figure 7) because of its stronger electron-

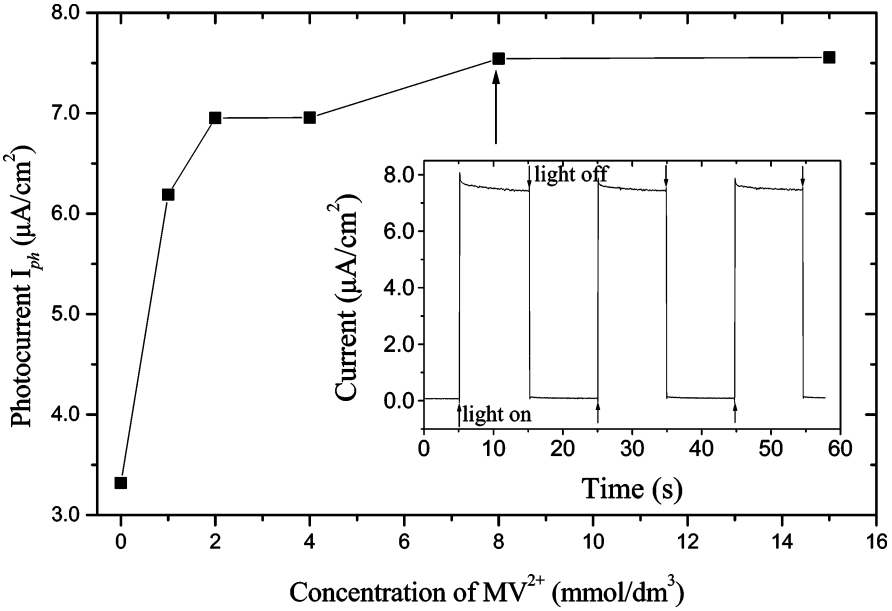

Figure 8. Influence of the MV^{2+} concentration on the short-circuit photocurrent (I_{sc}) of the monolayer LB films of P3HT−Dy@C_{82} (20:1) monolayers on ITO electrodes (0.1 mol·dm^{-3} KCl electrolyte solution, pH 6.5, white-light intensity = 354 mW·cm^{-2}). (Inset) Representative photocurrent trace vs time (no bias voltage, [MV^{2+}] = 8 mM). The arrows indicate the light on−off cycles.

accepting ability and higher concentration in the solution compared to the same properties of O_2. The leveling off of the photocurrent response at higher [MV^{2+}] indicates that the effect of the acceptor is saturated on the electrode surface.

Effect of Light Intensity. Figure 9 displays the linear response of the short-circuit photocurrent (I_{sc}) of the P3HT−Dy@C_{82} (20:1) monolayer film versus light intensity under the illumination of white light (A) and monochromatic light at 400 nm (B). No sign of photocurrent saturation was observed in the range of photon fluxes used in our experiments. This indicates an increasing population of charge carriers due to the more extensive excitation at higher light intensities and a unimolecular recombination process of the separated charges.[13,28] Similar results were obtained for the films of P3HT−C_{60} and pure P3HT. This is contrary to the PEC and PV cells based on thick films prepared by casting or spin coating,[5d,22] which generally exhibit a decrease in power-conversion efficiency (or quantum efficiency) with increasing illumination power. Such a deviation from linearity was ascribed to the recombination of charge carriers and/or charge trapping during the diffusion to the interfaces.[22] Thanks to the thinness of the LB films, however, our PEC cells can effectively hinder carrier recombination and trapping and therefore prevent the attendant loss of photocurrent efficiency.

I−V Curves at Different Compositions. Shown in Figure 10 are curves of photocurrent (I_{ph}) versus bias voltage (V_{bias}) for the monolayer films of P3HT−Dy@C_{82} (A) and P3HT−C_{60} (B) at different molar ratios in the presence of MV^{2+} under white-light illumination. When the P3HT monolayer films are doped with Dy@C_{82} (C_{60}), their photocurrent response is dramatically enhanced. Clearly, photoinduced charge transfer between P3HT and Dy@C_{82} (C_{60}) has occurred, which had already been revealed by the PL measurements (Figure 4). The fact that the cathodic photocurrent increases with increasing negative bias of the film electrode indicates that electrons flow from the ITO electrode through the LB film to the electrolyte, which is consistent with the p-type semiconducting nature of the polymer.[5] The largest enhancement is achieved for the film prepared at the molar ratio of P3HT/Dy@C_{82} = 20:1 (curve a in A).[17] For P3HT−C_{60}, the optimum molar ratio is P3HT/C_{60} = 25:1 (curve a in B). The pronounced composition dependence is more clearly seen in C for both I_{sc} and V_{oc}. The power-conversion efficiencies η_e of the PEC cells have been calculated from the data of I_{sc}, V_{oc}, and the fill factor (*FF*) (Table 2). One can see that up to a 16-fold enhancement in η_e is achieved for

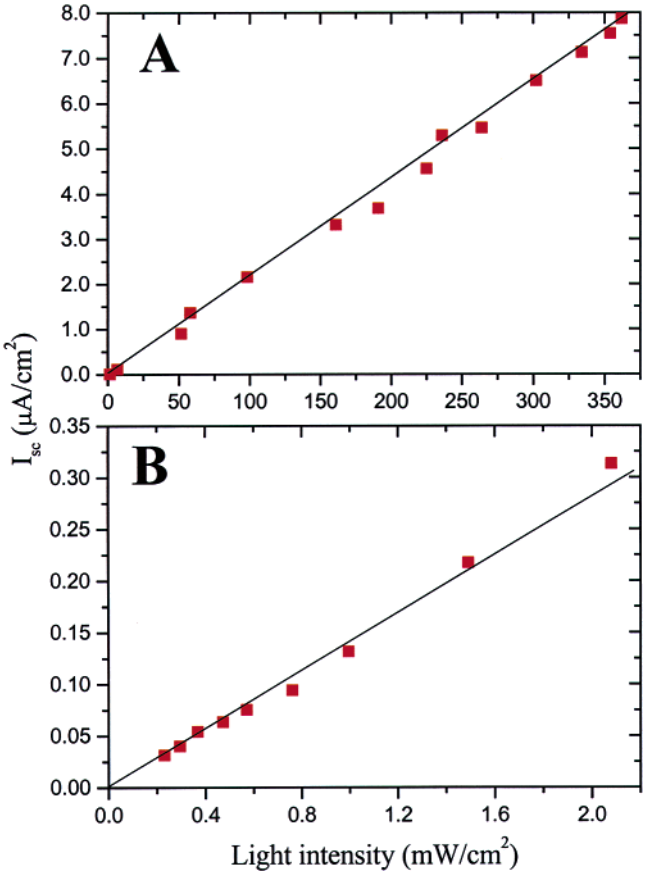

Figure 9. Dependence of the short-circuit photocurrent (I_{sc}) on the light intensity for P3HT−Dy@C_{82} (20:1) monolayers on ITO electrodes. (0.1 mol·dm^{-3} KCl electrolyte solution, pH 6.5, [MV^{2+}] = 8 mM) under the illumination of white light (A) and monochromatic light at 400 nm (B).

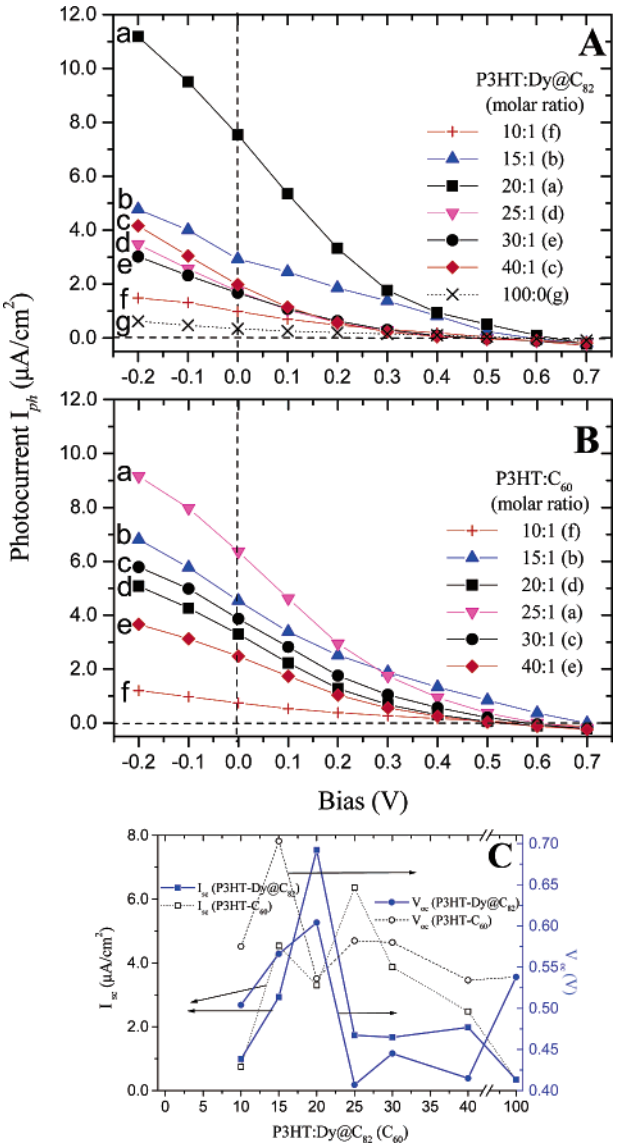

Figure 10. Photocurrent (I_{ph}) as a function of the electrode potential (V_{bias}) for the P3HT−Dy@C_{82} (A) and P3HT−C_{60} (B) monolayer LB films on ITO prepared at different molar ratios of P3HT/Dy@C_{82} (C_{60}) (0.1 mol·dm^{-3} KCl electrolyte solution, pH 6.5, [MV^{2+}] = 8 mM, intensity of white light = 354 mW·cm^{-2}). (C) I_{sc} and V_{oc} vs the molar ratio of P3HT/Dy@C_{82} (C_{60}).

the cell of P3HT/Dy@C_{82} = 20:1, which has the highest η_e of 1.9×10^{-4}% and is also somewhat higher than that of the P3HT−C_{60} (25:1) cell. To our knowledge, the enhancement is comparable to that reported for the PV cell based on P3HT and C_{60} derivatives.[16c] The single-wavelength photocurrent quantum yields are calculated according to $\Phi_\lambda = (I_{ph}/q)/(F_{abs})_\lambda$,[13,15] $(F_{abs})_\lambda = F_{i\lambda}(1-10^{-A_\lambda})$, where I_{ph} is the photocurrent (A cm^{-2}), q is the elementary charge in coulomb, $F_{i\lambda}$ is the incident photon flux (photons cm^{-2} s^{-1}), and A_λ is the film absorbance at wavelength λ. The results for λ = 400 nm are also tabulated in Table 2. Under our experimental conditions, the external quantum yield of the PEC cell, Φ_{400} (for λ = 400 nm) for P3HT/Dy@C_{82} = 20:1, is 3.88%, which is about an order of magnitude higher than that with pure P3HT and is also a bit higher than that of P3HT−C_{60} (25:1) (3.47%). It should be noted, however, that both η_e and Φ_{400} of our PEC cells are significantly lower than those of the recently developed P3HT/PCBM and MEH−PPV/PCBM PV cells.[16a,29] This is understandable because the P3HT−Dy@C_{82} monolayer in our PEC cells is as thin as 1 nm. Nevertheless, the comparison study demonstrates the effectiveness of the metallofullerene as an electron mediator for enhancing the photoelectric conversion.

By bringing the single-wavelength $I_{ph}-V_{bias}$ data into the $I_{ph}^2-V_{bias}$ plots (Supporting Information, Figure S1) and extrapolating the linear regions to zero, we obtain flat band potentials (E_{FB}), which are also tabulated in Table 2.[5c,30] Here, E_{FB} is the upper limit of a blocking potential region where the electrode response is dominated by the space−charge layer for p-type semiconductors.[5c,30] The values of E_{FB} are generally smaller than those reported for P3HT and its analogues,[5c,d] presumably because of the fact that our LB film is as thin as ~1 nm. Moreover, except for P3HT/Dy@C_{82} = 10:1, E_{FB} increases with the concentration of Dy@C_{82}, which can be explained by the partial charge transfer from P3HT to Dy@C_{82}. For P3HT−C_{60} films, E_{FB} is generally larger than that of the P3HT−Dy@C_{82} films, which is believed to be due to the different extent of charge transfer based on the different energy levels of C_{60} involved.

Effect of Film Morphology and Thickness. Because the encapsulation of Dy@C_{82} below the molar ratio of Dy@C_{82}/P3HT = 1:10 does not seem to modify the absorption characteristics of the film significantly in the visible region (Figure 2), the varied PEC performances of the films at different compositions are likely caused by the different molecular arrangements.[3a,31] This has been born out by the AFM measurements (Supporting Information, Figure S2). It is believed that at the optimum ratio of P3HT/Dy@C_{82} an ordered film structure is formed through $\pi-\pi$ interactions between the balls and the thiophene units, which quenches the self-aggregation of the constituent molecules. In this sense, both excessive and insufficient amounts of Dy@C_{82} will not ameliorate the film order because the molecules are more likely to self-aggregate.[17]

Figure 11 shows the film-thickness dependence of I_{sc}, η_e, and Φ for the P3HT−Dy@C_{82} (20:1) monolayer film under the illumination of white light (A) and monochromatic light at 400 nm (B). The cathodic photocurrent increases initially with an increasing number of layers but levels off at about seven layers. Two opposing factors should be considered here. For one, the increase in the number of photoactive molecules is expected to enhance the cathodic photocurrent. The other is the concomitant increase not only in the film's electrical resistance and charge trapping but also in the diffusion lengths for charge carriers, which would tend to decrease the photocurrent response. The deviation of the photocurrent from linearity versus the number of layers for thick films is believed to result from the balance of these two factors. Although the photocurrent displays an increasing deviation from linearity as a function of the number of layers, the photoabsorption keeps on increasing as the number of layers increases (Figure 5). This explains why both η_e and Φ exhibit maxima at three layers as seen in Figure 11.

Bilayer Cells. To understand the photocurrent-generation mechanism, we have examined bilayer PEC cells of ITO/P3HT/(Dy@C_{82}−AA)/MV^{2+} and ITO/(Dy@C_{82}−AA)/P3HT/MV^{2+}, where AA is arachidic acid (Dy@C_{82}/AA = 1:4).[32] The results are compared in Figure 12A. (See also Supporting Information, Figure S3.) In general, the photocurrent responses of the bilayer films are smaller than those of the corresponding composite films of P3HT−Dy@C_{82} with the same thickness (four layers) (Figure 11). This is understood by the reduced interfacial areas of the bilayer films compared with those of the composite films.[3a] Comparatively, the photocurrent responses of the ITO/(Dy@C_{82}−AA)/P3HT/MV^{2+} films (columns a−c) are about an order of magnitude higher than that of the ITO/P3HT/(Dy@C_{82}−

TABLE 2: Performances of the PEC Cells Based on P3HT/Dy@C_{82} (C_{60}) Monolayer LB Films on ITO Electrodes under Different Conditions

		white-light irradiation[b]						400-nm irradiation[c]			
film composition	ratio[a]	I_{pp} (μA/cm^2)	V_{pp} (V)	I_{sc} (μA/cm^2)	V_{oc} (V)	*FF*	η_e ($\times 10^{-4}$%)	I_{ph} (nA/cm^2)	abs[d]	Φ (%)	E_{FB}[e] (V)
P3HT−Dy@C_{82}	10:1	0.47	0.20	0.99	0.50	0.19	0.27	50	0.021	0.38	0.052
	15:1	1.38	0.30	2.93	0.57	0.25	1.17	168	0.018	1.50	0.132
	20:1	3.36	0.20	7.54	0.60	0.15	1.93	313	0.013	3.88	0.096
	25:1	0.56	0.20	1.73	0.41	0.16	0.32	86	0.016	0.86	0.081
	30:1	0.62	0.20	1.67	0.44	0.17	0.36	80	0.013	0.93	0.081
	40:1	1.14	0.10	1.98	0.42	0.14	0.32	89	0.018	0.79	0.053
P3HT−C_{60}	10:1	0.26	0.30	0.75	0.58	0.18	0.23	77	0.019	0.64	0.083
	15:1	1.89	0.30	4.54	0.70	0.18	1.63	326	0.017	3.04	0.134
	20:1	1.26	0.20	3.30	0.54	0.14	0.73	217	0.015	2.30	0.176
	25:1	2.95	0.20	6.54	0.58	0.16	1.69	379	0.017	3.47	0.178
	30:1	1.75	0.20	3.87	0.58	0.16	1.01	253	0.012	3.16	0.176
	40:1	1.02	0.20	2.48	0.53	0.15	0.58	136	0.014	1.47	0.157
pure P3HT	100:0	0.15	0.30	0.34	0.54	0.24	0.12	40	0.015	0.44	0.031

[a] Molar ratio of P3HT(unit): Dy@C_{82}. [b] Irradiation under white light of 354 mW/cm^2. [MV^{2+}] = 8 mM. Parameters: I_{pp}, V_{pp}, which are the current and voltage, respectively, at the peak power; I_{sc}: short-circuit current; V_{oc}: open-circuit voltage; *FF*: fill factor, $FF = (I_{pp}V_{pp})/(I_{sc}V_{oc})$; η_e: power-conversion efficiency. η_e % = $(I_{sc}V_{oc}FF)$/total incident energy × 100%. [c] Irradiation under 400-nm light of ~2.08 mW/cm^2. [MV^{2+}] = 8 mM. [d] Abs is the absorbance of the LB film at 400 nm. [e] Versus Ag/AgCl.

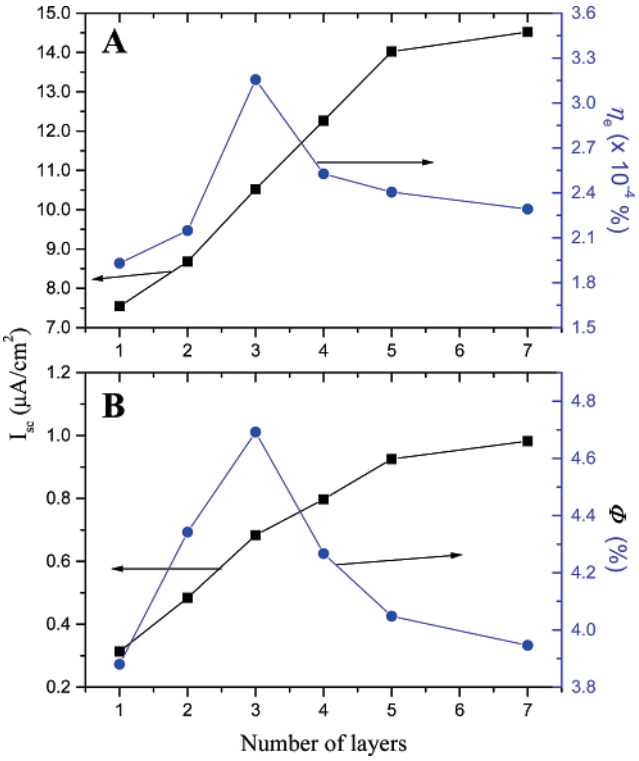

Figure 11. Dependence of I_{sc}, η_e, and Φ on the number of layers for P3HT−Dy@C_{82} (20:1) LB films on ITO electrodes (0.1 mol·dm^{-3} KCl electrolyte solution, pH 6.5, [MV^{2+}] = 8 mM) under the illumination of white light (A) and monochromatic light at 400 nm (B).

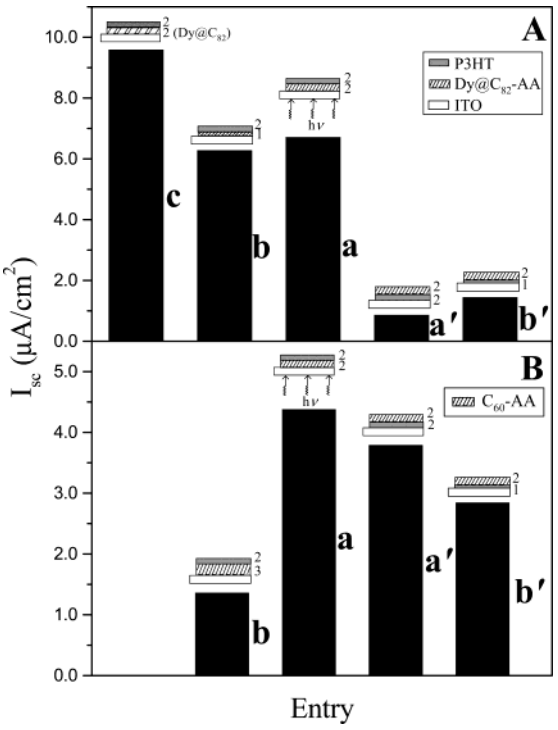

Figure 12. Dependence of I_{sc} on the structures and compositions of bilayer cells for P3HT−Dy@C_{82} (A) and P3HT−C_{60} (B) under white-light illumination (0.1 mol·dm^{-3} KCl electrolyte solution, pH 6.5, [MV^{2+}] = 8 mM, 354 mW·cm^{-2}). The numbers beside the blocks denote the number of layers for the LB films.

AA)/MV^{2+} film (columns a′−b′), indicating that the photoinduced electron transfer through the ITO-film−electrolyte path is more hindered in the latter case. By comparing columns a and b, it is found that doubling the (Dy@C_{82}−AA) layer thickness does not produce an appreciably higher photocurrent response. This suggests that the photocurrent response is dominated by the photoabsorption of P3HT, as also evidenced by the UV−vis spectra. (See Supporting Information, Figure S4.) Moreover, the ITO/Dy@C_{82}/P3HT/MV^{2+} cell (column c) exhibits a comparable (~90%) photocurrent response to that of a four-layer composite film (Figure 11). It is plausible that both systems share the same photoinduced charge-transfer pathway. For comparison, we also measured the bilayer films with Dy@C_{82} being replaced by C_{60} (Figure 12B). Similar results are obtained except that the photoinduced charge transfer from P3HT to C_{60} (columns a′−b′) can compete with the opposite process (columns a−b) (i.e., photoinduced electron transfer from C_{60} to P3HT, whereby the simultaneous excitation of both are needed). The different photocurrent responses of the bilayer cells made of C_{60} and Dy@C_{82} result from the fact the C_{60} is a poorer electron donor.[12c,13] Further discussion on the different photocurrent-generation mechanisms will follow.

Mechanistic Considerations. By using available data from the literature,[5d,12c,13,25] a schematic energy-level diagram for the ITO/(P3HT−Dy@C_{82})/MV^{2+} system can be constructed and is shown in Scheme 1. Note that the reduction and oxidation potentials of the metallofullerene are based on the solution data, and they may be somewhat different in the film states. Previously, we reported anodic photocurrent generation for the cells of ITO/(Dy@C_{82}−AA)/AsA (AA = arachidic acid; AsA = ascorbic acid) and ITO/(Dy@C_{82}−MPc)/AsA.[13,15] For the ITO/(P3HT−Dy@C_{82})/MV^{2+} cells, however, cathodic photocurrents are generated. Here, a quite different photocurrent-generation mechanism must be involved. According to the results of the present study, photocurrent generation must be started by the photoexcitation of P3HT. A plausible mechanism is proposed as follows:

$$\text{P3HT} + h\nu \rightarrow \text{P3HT*} \quad (1)$$

$$\text{P3HT*} + \text{MV}^{2+} \rightarrow \text{P3HT}^{+} + \text{MV}^{\bullet+} \quad (2)$$

$$\text{Dy@C}_{82} + \text{P3HT}^{+} \rightarrow \text{Dy@C}_{82}^{+} + \text{P3HT} \quad (3)$$

$$\text{Dy@C}_{82}^{+} + \text{CB}_{\text{ITO}} \rightarrow \text{Dy@C}_{82} + (\text{CB}_{\text{ITO}})^{+} \quad (4)$$

Photoexcited P3HT ($E_g \approx 2.0$ eV)[5d] passes the electron in the conduction band to electron acceptors MV^{2+} ($E^0_{MV^{2+}/MV^{\bullet+}} = -0.22$ V vs SCE) and/or O_2 ($E^0_{O_2/O_2^{\bullet-}} = -0.50$ V vs SCE at pH 7.0) in the electrolyte.[25,27,33] The P3HT molecule is replenished by an electron transferred from Dy@C_{82}, leaving behind a Dy@C_{82} cation ($E^0_{Dy@C_{82}^{+}/Dy@C_{82}} = 0.71$ V vs SCE).[13,15] Subsequently, the Dy@C_{82} cation is neutralized by the CB electron of ITO, completing the external circuit. It appears that Dy@C_{82} acts as a good electron mediator for passing the electron rapidly from ITO to P3HT. For C_{60}, however, electron transfer to P3HT may not be as facile because of its much weaker electron-donating ability ($E^0_{C_{60}^{+}/C_{60}} = 1.76$ V vs SCE) (Scheme 1).[15] In fact, in other work, we have also found that Dy@C_{82} is a better electron mediator than C_{60} in electrocatalytic reactions. This is apparently due to the fact that Dy@C_{82} is both a better electron donor and a better electron acceptor.[34] For C_{60}-based cells, apart from the photocurrent-generation pathway (eqs 1−4) described above (although C_{60}* may be involved here instead of C_{60}), another mechanism involving photoinduced electron transfer to C_{60}, which is known to occur in many polymer−C_{60} PV cells, should also be considered.[3a,b,16,29,35] This mechanism is embodied in the pathway (eqs 5−8) below.

$$\text{P3HT} + h\nu \rightarrow \text{P3HT*} \quad (5)$$

$$\text{P3HT*} + \text{C}_{60} \rightarrow \text{P3HT}^{+} + \text{C}_{60}^{-} \quad (6)$$

$$\text{C}_{60}^{-} + \text{MV}^{2+} \rightarrow \text{C}_{60} + \text{MV}^{\bullet+} \quad (7)$$

$$\text{P3HT}^{+} + \text{CB}_{\text{ITO}} \rightarrow \text{P3HT} + (\text{CB}_{\text{ITO}})^{+} \quad (8)$$

In terms of these mechanisms, the different photocurrent responses of the bilayer PEC cells (Figure 12) can be understood. For the Dy@C_{82}-based bilayer cells (Figure 12A), because of the energy-level alignments (Scheme 1), Dy@C_{82} can readily pass electrons from the ITO to P3HT*, but it is difficult to mediate electron transfer from P3HT* to MV^{2+}. Consequently, the photocurrent response of the ITO/(Dy@C_{82}−AA)/P3HT/MV^{2+} cell (columns a−c) is an order of magnitude higher than that of the ITO/P3HT/(Dy@C_{82}−AA)/MV^{2+} cell (columns a′−b′). In fact, for the latter case, the photoexcitation of Dy@C_{82} may be needed to generate the cathodic photocurrent. This explains why the photocurrent decreases with the thickness of P3HT, which is accompanied by the decreasing absorption of Dy@C_{82}. C_{60}-based bilayer cells (Figure 12B) show quite different photocurrent responses because of the different energy-level alignments (Scheme 1). Although C_{60} can now pass electrons from P3HT* to MV^{2+}, its transfer of electrons to P3HT* needs to be assisted by photoexcitation, which is more favorable than that of Dy@C_{82} (Figure S4). The two photocurrent-generation mechanisms are competitive, leading to comparable photocurrent responses for the ITO/(C_{60}−AA)/P3HT/MV^{2+} (columns a−b) and ITO/P3HT/(C_{60}−AA)/MV^{2+} (columns a′−b′) cells of appropriate thickness. In the former case, increasing the C_{60}−AA layer thickness decreases the absorption of P3HT; therefore, the photocurrent decreases. For the latter, however, increasing the P3HT layer thickness increases the photocurrent simply because more activated P3HT* molecules are generated.

SCHEME 1: Schematic Representation of the Electron-Transfer Processes for Cathodic Photocurrent Generation

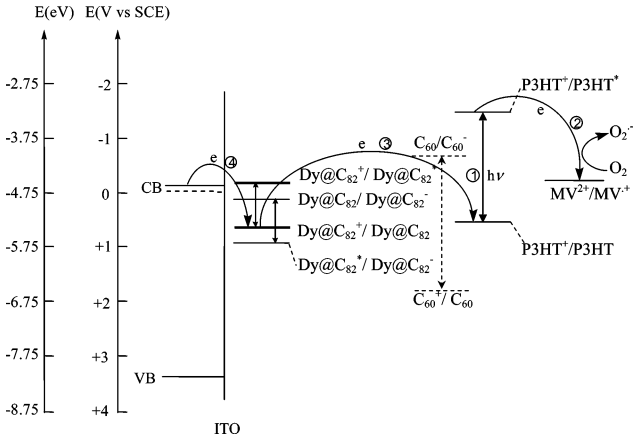

Conclusions

PEC cells based on the LB films of P3HT doped with Dy@C_{82} have been successfully constructed and characterized. The Langmuir films are proposed to assemble in such a way that the Dy@C_{82} molecules are partially inserting into the chain matrix of P3HT with the polymer backbones taking an edge-on arrangement (i.e., the aromatic rings are perpendicular to the air/water interface). A dramatic enhancement of the stable cathodic photocurrent has been demonstrated for the PEC cells prepared by dispersing Dy@C_{82} (C_{60}) into the LB films of P3HT, with η_e and Φ being up to 16-fold and 9-fold higher, respectively, than the same parameters for those made of pure P3HT. This is attributed to the facile photoinduced electron transfer between P3HT and Dy@C_{82} (C_{60}), which is supported by the PL measurements. We have revealed the correlation of the optimum ratio for the PEC performance with the ordered film structure, which appears to be the basis for the facile photoinduced electron transfer. The effects of the electron acceptor, bias voltage, light intensity, and number of layers have been studied in detail. Together with the studies on the bilayer PEC cells, a reasonable photocurrent-generation mechanism has been proposed, which starts with the photoabsorption of P3HT followed by electron transfer to MV^{2+} and hole transfer to ITO through Dy@C_{82}. The comparative study on C_{60} suggests that a different photocurrent-generation mechanism, which involves the photoinduced electron transfer from P3HT to C_{60}, can also be competitive. We believe that this study provides not only fundamental insight into the PEC cells based on conducting

polymer−fullerene composites but also important information for the design of future plastic solar cells.

Acknowledgment. This work was supported by an RGC grant administered by the UGC of Hong Kong. We thank Mr. C. L. Yang for PL measurements and MCPF of HKUST for AFM measurements.

Supporting Information Available: Single-wavelength $I_{ph}^2-V_{bias}$ plots, AFM images of P3HT−Dy@C_{82} monolayer LB films with different compositions, photocurrent response curves of bilayer cells, and representative UV−vis absorption spectra of bilayer films. This material is available free of charge via the Internet at http://pubs.acs.org.

References and Notes

(1) Schopf, G.; Koβmehl, G. *Polythiophenes*: *Electrically Conductive Polymers*; Springer: Berlin, 1997.

(2) (a) Zhou, Q.; Swager, T. M. *J. Am. Chem. Soc.* **1995**, *117*, 12593. (b) McCullough, R. D. *Adv. Mater.* **1998**, *10*, 93.

(3) (a) Brabec, C. J.; Sariciftci, N. S.; Hummelen, J. C. *Adv. Funct. Mater.* **2001**, *11*, 15. (b) Wallace, G. G.; Dastoor, P. C.; Officer, D. L.; Too, C. O. *Chem. Innovation* **2000**, *30*, 14. (c) Hagfeldt, A.; Grätzel, M. *Acc. Chem. Res.* **2000**, *33*, 269.

(4) (a) Grätzel, M. *Nature* **2001**, *414*, 338. (b) Santhanam, K. S. V.; Sharon, M. *Photoelectrochemical Solar Cells*; Elsevier: Amsterdam, 1988. (c) Aruchamy, A. *Photoelectrochemistry and Photovoltaics of Layered Semiconductors*; Kluwer Academic: Dordrecht, The Netherlands, 1992.

(5) (a) Miquelino, F. L. C.; De Paoli, M. A.; Genies, E. M. *Synth. Met.* **1994**, *68*, 91. (b) Micaroni, L.; Dini, D.; Decker, F.; De Paoli, M. *Electrochim. Acta* **1998**, *44*, 753. (c) Girotto, E. M.; Gazotti, W. A.; De Paoli, M. A. *J. Phys. Chem. B* **2000**, *104*, 6124. (d) El-Rashiedy, O. A.; Holdcroft, S. *J. Phys. Chem.* **1996**, *100*, 5481.

(6) (a) Xu, G. F.; Bao, Z. N.; Groves, J. T. *Langmuir* **2000**, *16*, 1834. 7. (b) Bao, Z. N.; Dodabalapur, A.; Lovinger, A. J. *Appl. Phys. Lett.* **1996**, *69*, 4108.

(7) (a) Rikukawa, M.; Nakagawa, M.; Ishida, K.; Abe, H.; Sanui, K.; Ogata, N. *Thin Solid Films* **1996**, *284*, 636. (b) Malhotra, B. D.; Takashima, W.; Pandey, S. S.; Singhal, R.; Endo, K.; Rikukawa, M.; Kaneto, K. *Jpn. J. Appl. Phys.* **1999**, *38*, 6768. (c) Watanable, I.; Hong, K.; Rubner, M. F. *Langmuir* **1990**, *6*, 1164. (d) Liu, Y. Q.; Xu, Y.; Zhu, D. B. *Synth. Met.* **1997**, *90*, 143. (e) Ahlskog, M.; Paloheimo, J.; Stubb, H.; Dyreklev, P.; Fahlman, M.; Inganäs, O.; Andersson, M. R. *J. Appl. Phys.* **1994**, *76*, 893. (f) Pal, A. J.; Östergard, T.; Paloheimo, J.; Stubb, H. *Appl. Phys. Lett.* **1996**, *69*, 1137. (g) Pal, A. J.; Östergard, T. P.; Österbacka, R. M.; Paloheimo, J.; Stubb, H. *IEEE J. Sel. Top. Quantum Electron* **1998**, *4*, 137.

(8) (a) Bjφrnholm, T.; Hassenkam, T.; Greve, D. R.; McCullough, R. D.; Jayaraman, M.; Savoy, S. M.; Jones, C. E.; McDevitt, J. T. *Adv. Mater.* **1999**, *11*, 1218. (b) Hassenkam, T.; Greve, D. R.; Bjφrnholm, T. *Adv. Mater.* **2001**, *13*, 631. (c) Bjφrnholm, T.; Hassenkam, T.; Reitzel, N. *J. Mater. Chem.* **1999**, *9*, 1975. (d) Reitzel, N.; Greve, D. R.; Kjaer, K.; Howes, P. B.; Jayaraman, M.; Savoy, S. M.; McCullough, R. D.; McDevitt, J. T.; Bjφrnholm, T. *J. Am. Chem. Soc.* **2000**, *122*, 5788.

(9) (a) Luo, C. P.; Guldi, D. M.; Maggini, M.; Menna, E.; Mondini, S.; Kotov, N. A.; Prato, M. *Angew. Chem., Int. Ed.* **2000**, *39*, 3905. (b) Barazzouk, S.; Hotchandani, S.; Kamat, P. V. *Adv. Mater.* **2001**, *13*, 1614.

(10) Licht, S.; Khaselev, P. A.; Ramakrishnan, P. A.; Faiman, D.; Katz, E. A.; Shames, A.; Goren, S. *Sol. Energy Mater. Sol. Cells* **1998**, *51*, 9.

(11) (a) Shinohara, H. *Rep. Prog. Phys.* **2000**, *63*, 843 and references therein. (b) Yang, S. H. *Trends Chem. Phys*. **2001**, *9*, 31.

(12) (a) Allemand, P. M.; Koch, A.; Wudl, F.; Rubin, Y.; Diederich, F.; Alvarez, M. M.; Anz, S. J.; Whetten, R. L. *J. Am. Chem. Soc.* **1991**, *113*, 1050. (b) Suzuki, T.; Maruyama, Y.; Akasaka, T.; Ando, W.; Kobayashi, K.; Nagase, S. *J. Am. Chem. Soc.* **1994**, *116*, 1359. (c) Wang, W. L.; Ding, J. Q.; Yang, S. H.; Li, X. Y. *Electrochem. Soc. Proc.* **1997**, 97−14, 417.

(13) Yang, S. F.; Yang, S. H. *J. Phys. Chem. B* **2001**, *105*, 9406 and references therein.

(14) (a) Huang, H. J.; Yang, S. H. *J. Organomet. Chem*. **2000**, *599*, 42. (b) Huang. H. J.; Yang, S. H. Film Formation Behavior of the Endohedral Metallofullerene Dy@C_{82}. In *Amorphous and Nanostructured Carbon*; Robertson, J., Sullivan, J. P., Zhou, O., Allen, T. B., Coll, B. F., Eds.; Materials Research Society: Boston, 2000; Vol. 593, pp 63−68. (c) Li, X. G.; Yang, S. F.; Yang, S. H.; Xu, Y.; Liu, Y. Q.; Zhu, D. B. *Thin Solid Films* **2002**, *413*, 231.

(15) Yang, S. F.; Fan, L. Z.; Yang, S. H. *J. Phys. Chem. B* **2003**, *107*, 8403.

(16) (a) Padinger, F.; Rittberger, R. S.; Sariciftci, N. S. *Adv. Funct. Mater.* **2003**, *13*, 85. (b) Camaioni, N.; Ridolfi, G.; Casalbore-Miceli, G.; Possamai, G.; Maggini, M. *Adv. Mater.* **2002**, *14*, 1735. (c) Camaioni, N.; Garlaschelli, L.; Geri, A.; Maggini, M.; Possamai, G.; Ridolfi, G. *J. Mater. Chem.* **2002**, *12*, 2065.

(17) Yang, S. F.; Fan, L. Z.; Yang, S. H. *Chem. Phys. Lett.*, in press.

(18) (a) Huang, H. J.; Yang, S. H. *J. Phys. Chem. B* **1998**, *102*, 10196. (b) Gu, G.; Huang, H. J.; Yang, S. H.; Yu, P.; Fu, J.; Wong, G. K. L.; Wan, X.; Dong, J.; Du, Y. *Chem. Phys. Lett.* **1998**, *289*, 167.

(19) Smolenyak, P. E.; Osburn, E. J.; Chen, S.-Y.; Chau, L.-K.; O'Brien, D. F.; Armstrong, N. R. *Langmuir* **1997**, 65688.

(20) Note that this definition of *R* is different from that described in ref 6a. See also (a) Rikuruwa, M.; Rubner, M. F. *Langmuir* **1994**, *10*, 519. (b) Kani, R.; Nakano, Y.; Majima, Y.; Hayase, S.; Yuan, C. H.; West, R. *Macromolecules* **1994**, *27*, 1911.

(21) (a) Dyreklev, P.; Inganäs, O.; Paloheimo, J.; Stubb, H. *J. Appl. Phys.* **1992**, *71*, 2816. (b) Jiang, X. M.; Österbacka, R.; Korovyanko, O.; An, C. P.; Horovitz, B.; Janssen, R. A. J.; Vardeny, Z. V. *Adv. Funct. Mater.* **2002**, *12*, 587. (c) Korovyanko, O. J.; Österbacka, R.; Jiang, X. M.; Vardeny, Z. V. *Phys. Rev. B* **2001**, *64*, 235122.

(22) (a) Roman, L. S.; Andersson, M. R.; Yohannes, T.; Inganäs, O. *Adv. Mater.* **1997**, *9*, 1164. (b) Sariciftci, N. S.; Smilowitz, L.; Heeger, A. J.; Wudl, F. *Science* **1992**, *258*, 1474. (c) Sariciftci, N. S.; Braun, D.; Zhang, C.; Srdanov, V. I.; Heeger, A. J.; Stucky, G.; Wudl, F. *Appl. Phys. Lett.* **1993**, *62*, 585. (d) Sariciftci, N. S.; Heeger, A. J. *Int. J. Mod. Phys. B* **1994**, *8*, 237.

(23) Theander, M.; Yartsev, A.; Zigmantas, D.; Sundström, V.; Mammo, W.; Andersson, M. R.; Inganäs, O. *Phys. Rev. B* **2000**, *61*, 12957.

(24) (a) Lee, S. B.; Zakhidov, A. A.; Khairullin, I. I.; Sokolov, V. Y.; Khabibullaev, P. K.; Tada, K.; Yoshimoto, K.; Yoshino, K. *Synth. Met.* **1996**, *77*, 155. (b) Hasharoni, K.; Keshavarz-K, M.; Sastre, A.; González, R.; Bellavia-Lund, C.; Greenwald, Y.; Swager, T.; Wudl, F.; Heeger, A. J. *J. Chem. Phys.* **1997**, *107*, 2308.

(25) (a) Zhang, W.; Shi, Y. R.; Gan, L. B.; Huang, C. H.; Luo, H. X.; Wu, D. G.; Li. N. Q. *J. Phys. Chem. B* **1999**, *103*, 675. (b) Wu, D. G.; Huang, C. H.; Gan, L. B.; Zhang, W.; Zheng, J.; Luo, H. X.; Li, N. Q. *J. Phys. Chem. B* **1999**, *103*, 4377. (c) Imahori, H.; Yamada, H.; Nishimura, I.; Sakata, Y. *J. Phys. Chem. B* **2000**, *104*, 2099.

(26) Abdou, M. S. A.; Holdcroft, S. *Macromolecules* **1993**, *26*, 2954.

(27) Hoare, J. P. In *Standard Potentials in Aqueous Solution*; Bard, A. J., Parsons, R., Jordan, J., Eds.; Marcel Dekker: New York, 1985; Chapter 4.

(28) Donovan, K. J.; Sudiwala, R. V.; Wilson, E. G. *Mol. Cryst. Liq. Cryst.* **1991**, *194*, 337.

(29) Yu, G.; Gao, J.; Hummelen, J. C.; Wudl, F.; Heeger, A. J. *Science* **1995**, *270*, 1789.

(30) Finklea, H. O. *Semiconductor Electrodes*; Elsevier: New York, 1988.

(31) Moons, E. *J. Phys: Condens. Matter* **2002**, *14*, 12235.

(32) Different deposition sequences of the P3HT and (Dy@C_{82}-AA) layers are distinguished by the order. The bracket represents a two-component mixture that is deposited in one layer. For bilayer cells, the symbol / denotes the interface.

(33) Kim, Y. S.; Liang, K.; Law, K. Y.; Whitten, D. G. *J. Phys. Chem. B* **1994**, *98*, 984.

(34) Fan, L. Z.; Yang, S. F.; Yang, S. H. *Langmuir*, in press.

(35) (a) Fromherz, T.; Padinger, F.; Gebeyehu, D.; Brabec, C.; Hummelen, J. C.; Sariciftci, N. S. *Sol. Energy Mater. Sol. Cells* **2000**, *63*, 61. (b) Brabec, C. J.; Cravino, A.; Zerra, G.; Sariciftci, N. S.; Kiebooms, R.; Vanderzande, D.; Hummelen, J. C. *J. Phys. Chem. B* **2001**, *105*, 1528.